Weakly non-parallel stability of a condensing film flow

Simeon Djambov[1], François Gallaire[1]

[1] Laboratory of Fluid Mechanics and Instabilities, École Polytechnique Fédérale de Lausanne, 1015 Lausanne, Switzerland
Corresponding author: simeon.djambov@epfl.ch

A quiescent, saturated vapour condenses onto a uniformly cooled, inclined plate and forms a laminar, incompressible, gravity-driven film flow of a Newtonian liquid of constant material properties (fig. 1). We make the problem dimensionless by rescaling all distances with a characteristic length H_N, to be determined; we use a Nusselt velocity scale, a hydrostatic pressure scale, and recast the temperature field from 0 on the wall to 1 on the interface. The system is governed by the incompressible Navier–Stokes and heat equations

$$\boldsymbol{\nabla} \cdot \boldsymbol{u} = \boldsymbol{0}, \tag{1}$$

$$Re(\partial_t \boldsymbol{u} + \boldsymbol{u} \cdot \boldsymbol{\nabla} \boldsymbol{u}) = -\boldsymbol{\nabla} p + \boldsymbol{f} + \nabla^2 \boldsymbol{u}, \tag{2}$$

$$Pe(\partial_t T + \boldsymbol{u} \cdot \boldsymbol{\nabla} T) = \nabla^2 T, \tag{3}$$

where $\boldsymbol{u}$ is the two-dimensional velocity field, p is the pressure, and T is the temperature; $\boldsymbol{f} = \hat{\boldsymbol{x}} - \cot\theta \hat{\boldsymbol{y}}$ is the gravity forcing. The Reynolds number $Re = \rho^2 g \sin\theta H_N^2/\mu^2$ compares inertial and viscous effects and the Péclet number $Pe = \rho g \sin\theta H_N^3/(\mu\kappa) = PrRe$ is the ratio of thermal advection to thermal diffusion, related to the Reynolds number through the Prandtl number Pr.

No-slip and no-penetration conditions, as well as a constant temperature are imposed at the substrate, $y = 0$. We consider conditions, in which the phase change takes place in a quasi-equilibrium. Hence the temperature of the interface is constant and equal to the saturation condensation temperature. Further, we perform our analysis in the framework of the one-sided model, whereby we consider the vapour phase as mechanically passive [1]. The liquid–vapour interface, $y = h(x)$, is thus free of tangential stress and undergoes a curvature-induced jump in the normal stress, $We\partial_{xx}^2 h/(1 + (\partial_x h)^2)^{3/2}$. The Weber number $We = \gamma/(\rho g \sin\theta H_N^2)$ compares capillary to hydrostatic pressures.

The set of governing equations is completed by the kinematic boundary condition of the free surface, or equivalently the mass conservation equation

$$\partial_t h + \boldsymbol{u} \cdot \boldsymbol{\nabla}[h - y]\big|_{y=h} = -\frac{Ja}{Pe} \boldsymbol{\nabla} T \cdot \boldsymbol{\nabla}[h - y]\big|_{y=h}, \tag{4}$$

where $Ja = c_p(T_\infty - T_w)/h_{lv}$ is the Jakob number, which measures the ratio of sensible to latent heats.

For most liquids of interest, including water, the steady basic flow is to a very good approximation the one derived by Nusselt (1916) [2]. The flow fields are all adiabatically slaved to the film thickness $h_0(x)$ and

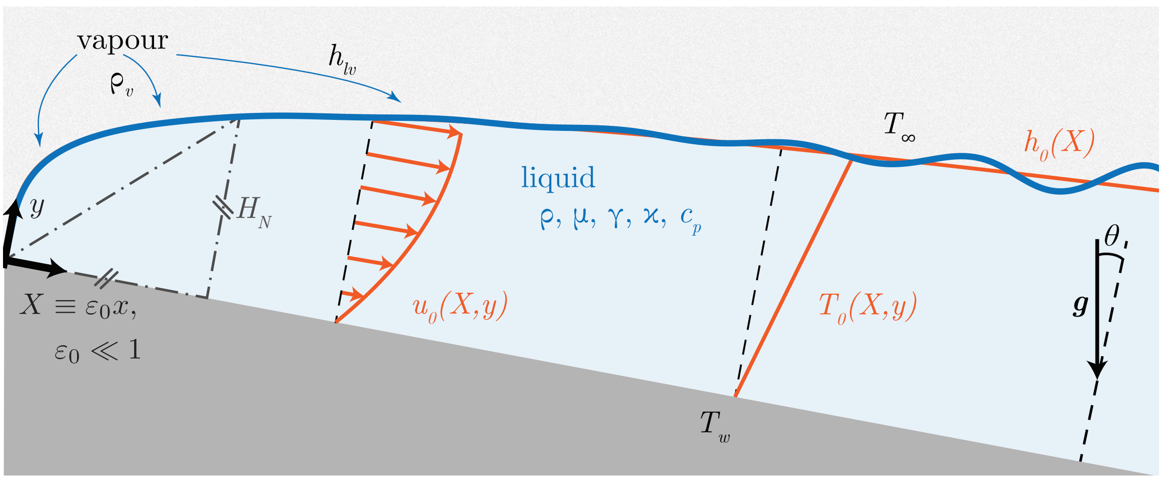

Figure 1: Sketch of the problem at hand. The basic flow is depicted in orange.

involve a half-parabolic velocity, linear pressure, and linear temperature profiles in the wall-normal direction

$$h_0(x) = x^{1/4}, \tag{5}$$

$$\boldsymbol{u_0}(x,y) = y(h_0(x) - y/2)\hat{\boldsymbol{x}} - h_0'(x)y^2/2\hat{\boldsymbol{y}}, \tag{6}$$

$$p_0(x,y) = \cot\theta(h_0(x) - y), \tag{7}$$

$$T_0(x,y) = y/h_0(x), \tag{8}$$

where we have chosen a length scale such that *Pe* $= 4$*Ja*,

$$H_N = \left(\frac{4\mu\kappa c_p(T_\infty - T_w)}{\rho g \sin\theta h_{lv}}\right)^{1/3}. \tag{9}$$

This choice can be geometrically interpreted as the equality of the streamwise position with the film thickness at that position (see fig. 1).

We seek to establish the system's linear response to a harmonic forcing of real angular frequency ω. We are interested in the onset of Kapitza waves on the condensing film's surface [3]. The problem's well-posedness is ensured by the convective nature of the Kapitza instability. The basic flow's slow dependence on the streamwise coordinate, $h_0'(x \to \infty) \to 0$, enables the use of the Wentzel–Kramers–Brillouin–Jeffreys (WKBJ) formalism [4]. The linear perturbations take the form

$$\boldsymbol{q}(x,y,t) \sim A(X)\tilde{\boldsymbol{q}}(y;X)\exp\left[\mathrm{i}\left(\varepsilon_0^{-1}\int_{X_0}^{X} k(\omega;X')\mathrm{d}X' - \omega t\right)\right] + \text{c.c.}, \tag{10}$$

where the local eigenfunctions $\tilde{\boldsymbol{q}} = (\tilde{\boldsymbol{u}}, \tilde{p}, \tilde{T}, \tilde{h})$ contain the state variables and $X \equiv \varepsilon_0 x$ is the slow streamwise coordinate with $\varepsilon_0 \ll 1$, which is a measure of the basic flow's weak non-parallelism. The local complex wave number $k(\omega; X')$ is associated to the frequency ω, at the streamwise section X'; its negative imaginary part is the local spatial growth rate. It is computed from the linearised governing equations at leading order in ε_0, *i*.e. over a quasi-parallel slice of the basic flow. The slowly-varying, complex envelope function $A(X)$ smoothly stitches the local spatial stability analyses. It is obtained from a solvability condition at first order in ε_0, where the slow evolution of both the basic flow and of the local spatial dispersion relations are taken into account. Imposing $A(X_0) = 1$ as initial condition, describes a localised forcing with the local eigenfunction $\tilde{\boldsymbol{q}}(y; X_0)$. The geometry of the problem lacks a proper inlet and X_0 is the arbitrary position, where a disturbance could force the system.

Indeed, as regards the system's local linear stability, a unique spatial branch, associated to downstream-propagating waves, becomes unstable (fig. 2a). Compared to the classical Kapitza instability of an isothermal, uniform film flow, where destabilising inertia competes against the stabilising effects of gravity and capillarity, the condensing film flow is additionally locally stabilised by the phase change: as thinner liquid layers promote heat transfer, eq. (8), vapour tends to condense more in the perturbation's troughs rather than on the crests, thus damping perturbations. Nevertheless, since the basic film thickness grows, eq. (5), inertia experienced by perturbations increases downstream and after a critical distance x^c, Kapitza waves can develop. Note that the wavelength of the first locally linearly unstable perturbation is much smaller than the basic flow evolution length scale at the same location, for the example of fig. 2a $k^* \approx 4 \times 10^{-3} \gg 4 \times 10^{-5} \approx h_0'(x)/h_0(x) = 0.25x^{-1}$. This is systematically the case and makes the weakly non-parallel approach suitable. Marginal stability is attained for considerably higher local Reynolds numbers $Re_x = Re\,h_0^3(x)$ than for the non-condensing case. Increasing the Jakob number *Ja*, *i*.e. a cooler plate, requires a thicker film for the onset of instability. However, this also makes the basic flow thicken – and hence, reach local linear instability – faster, *i*.e. in a shorter dimensional distance (fig. 2b).

Finally, in order to predict the linearly prevalent frequency, we consider the amplification of locally present noise. The gain is defined as the squared modulus of the linear perturbation, eq. (10),

$$G^2(L, X_0; \omega) = |A(L)|^2 \exp\left[-2\int_{X_0}^{L} k_i(\omega; X')\mathrm{d}X'\right], \tag{11}$$

where k_i is the imaginary part of the wave number, *i*.e. the negative local spatial growth rate. It consists in an accumulation of the local growth rates, corrected for the weak non-parallelism by the WKBJ amplitude (presented separately in fig. 3 for $X_0 = 1$). Upstream of the critical distance x^c, all perturbations are damped. Higher frequencies are subject to more severe attenuation and over a longer distance, but tend to grow faster

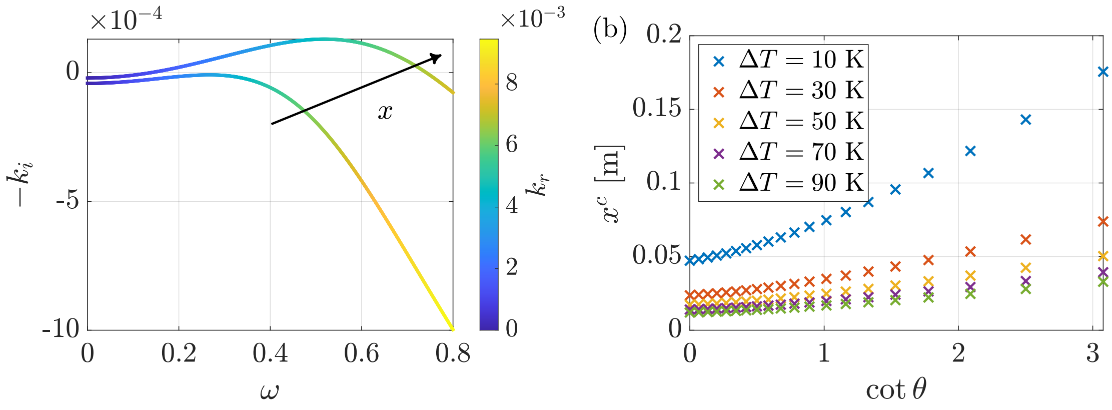

Figure 2: (a) $\theta = \pi/4$, $Ja \approx 0.02$, $We \approx 8 \times 10^4$, $Pr \approx 7$. Examples of stable and unstable spatial dispersion relations at streamwise sections $x = \{6 \times 10^3, 1.2 \times 10^4\}$ (in dimensional quantities, for water, condensing on an incline of $\pi/4$ with an imposed cooling of 10 K, these scale to around 7 and 14 cm; the film is around 100 and 120 μm thick). (b) Dimensional critical distance as a function of the inclination angle θ for several imposed temperature differences $\Delta T \equiv T_\infty - T_w$, material properties of water.

afterwards. The weakly non-parallel correction remains inferior to 1, which captures the non-optimal projection of perturbations on the local eigenfunctions of following slices. It also exhibits a non-monotonic behaviour, which indicates the presence, although minor, of non-parallel instability mechanisms, overlooked by the local stability analyses. Remark the radical difference in scale of the ordinates; the accumulation of local spatial growth rates is by far the main contribution to the gain.

The competition, which would settle the linear frequency selection, has two aspects: on the one hand, larger frequencies take longer to become unstable, while on the other hand, once unstable, they tend to grow faster. Figure 4 presents the gain, eq. (11), as a function of plate length L and frequency ω with a forcing location X_0, optimised for each frequency ω. This optimal forcing location is found at the minimum of the gain, as in this way perturbations can avoid the upstream damping region, while benefiting from the longest possible region of sustained growth. It is almost equal to the critical streamwise distance for local linear instability x^c, only slightly modulated by the amplitude $|A(L)|$. Before this minimum, *i*.e. before perturbations can start growing, the maximum attainable gain is 1, resulting from a forcing located at the position of interest itself.

After setting a threshold for nonlinear saturation (in other words, an external perturbation amplitude, assuming nonlinearities kick in for amplitudes equal to one), our analysis results in a prediction for the Kapitza waves frequency. For example, $G^2_{\text{sat}} = 10^{10}$ is first reached by a forcing of angular frequency 0.88. In dimensional quantities, for water, condensing on an incline of $\pi/4$ with an imposed cooling of 10 K, waves of frequency 11 Hz should saturate after around 46 cm. If the threshold is higher, *e*.g. thanks to lower ambient noise levels,

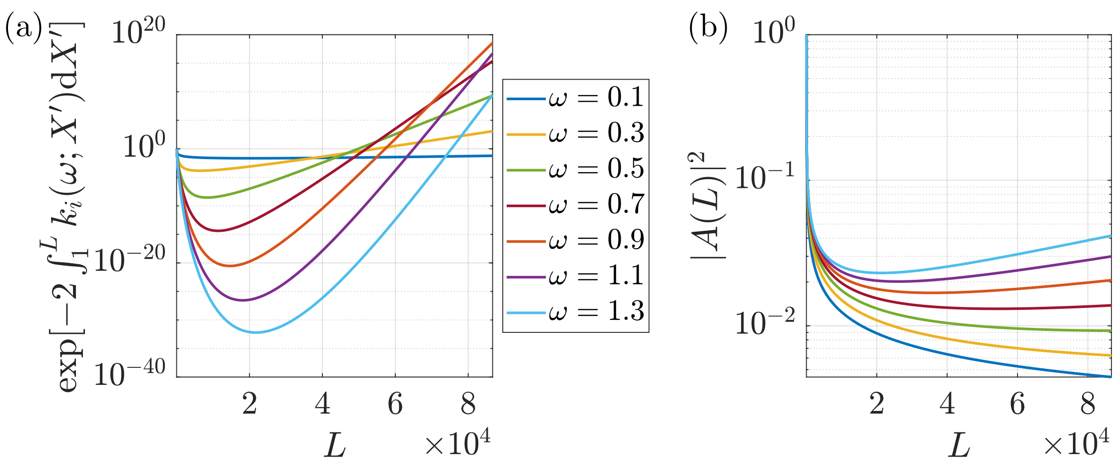

Figure 3: $\theta = \pi/4$, $Ja \approx 0.02$, $We \approx 8 \times 10^4$, $Pr \approx 7$, $X_0 = 1$. (a) Leading-order spatial gain. (b) WKBJ amplitude. The legend is common for both panels.

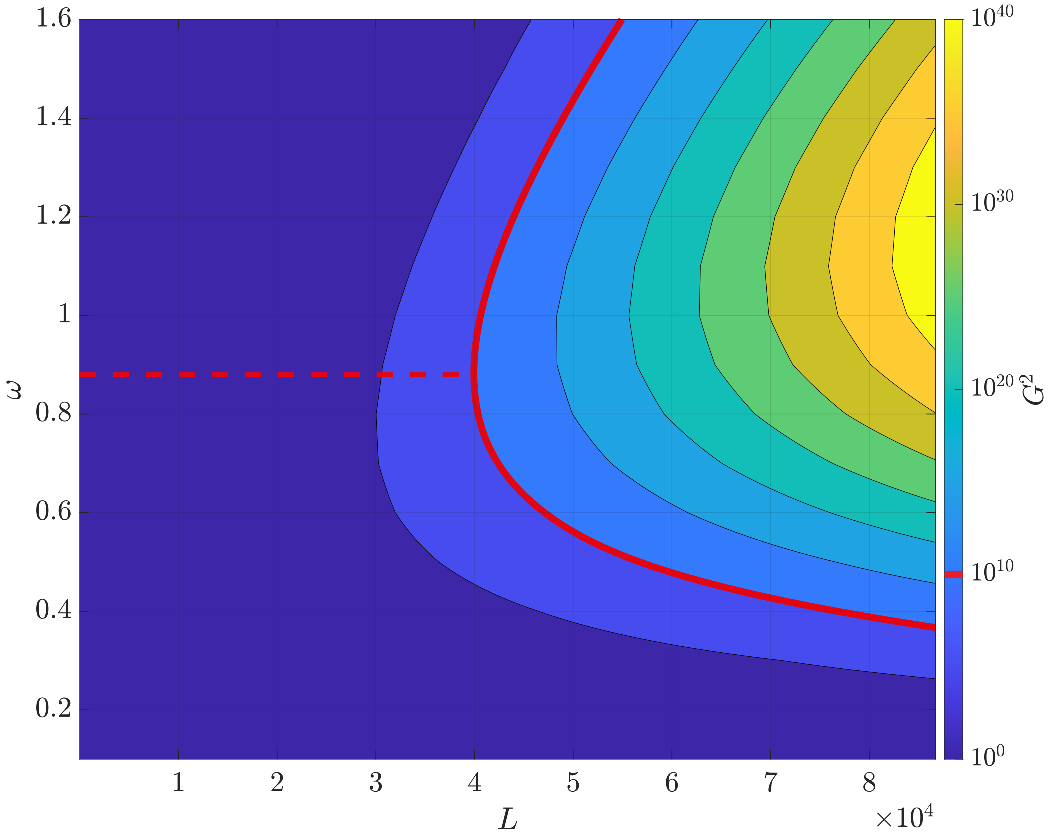

Figure 4: $\theta = \pi/4$, $Ja \approx 0.02$, $We \approx 8 \times 10^4$, $Pr \approx 7$. Optimal locally-forced gain as a function of plate length and frequency. The red solid line follows an isoline of $G^2 = 10^{10}$.

the predicted most amplified frequency increases.

Thereafter, a more realistic, spatially-distributed forcing can be considered in order to eventually improve the prediction. Our analysis can also be extended to other weakly non-parallel flows, for example the rain-fed film flow, which thickens as $x^{1/3}$.

References

[1] A. Oron, S. H. Davis, and S. G. Bankoff, *Rev. Mod. Phys.* **69**(3), 931–980 (1997).

[2] W. Nusselt, *Z. Ver. Dtsch. Ing.* **60**(27), 541–546 (1916).

[3] P. L. Kapitza, *Zh. Eksp. Teor. Fiz.* **18**, 3–18 (1948).

[4] P. Huerre and M. Rossi, Hydrodynamic instabilities in open flows, *Hydrodynamics and nonlinear instabilities* / C. Godrèche and P. Manneville, (Cambridge University Press, 1998).